Published in final edited form as:
Free Radic Biol Med. 2011 December 1; 51(11): 1975–1984. doi:10.1016/j.freeradbiomed.2011.08.022.

Novel Insights Into Interactions Between Mitochondria and Xanthine Oxidase in Acute Cardiac Volume Overload

James D Gladden, BS[1,5], **Blake R Zelickson, BS**[1,3,4], **Chih-Chang Wei, PhD**[1,2,6], **Elena Ulasova, PhD**[1,3,4], **Junying Zheng, PhD**[1,2], **Mustafa I. Ahmed, MD**[1,2], **Yuanwen Chen, MD, PhD**[1,2], **Marcas Bamman, PhD**[5,6], **Scott Ballinger, PhD**[1,3,4], **Victor Darley-Usmar, PhD**[1,3,4], and **Louis J Dell'Italia, MD**[1,2,4,6]

[1]UAB Center for Heart Failure Research, University of Alabama at Birmingham

[2]Department of Medicine, University of Alabama at Birmingham

[3]Department of Pathology, University of Alabama at Birmingham

[4]Center for Free Radical Biology, University of Alabama at Birmingham

[5]Department of Physiology and Biophysics, University of Alabama at Birmingham

[6]Department of Veterans Affairs Medical Center, Birmingham, Alabama

Abstract

Xanthine oxidoreductase (XOR) is increased in the left ventricle (LV) of humans with volume overload (VO) and mitochondrial inhibition of the respiratory chain occurs in animal models of VO. Since mitochondria are both a source and target of reactive oxygen and nitrogen species, we hypothesized that activation of XOR and mitochondrial dysfunction are interdependent. To test this we used the aortocaval fistula (ACF) rat model of VO and a simulation of the stretch response in isolated adult cardiomyocytes with and without the inhibitor of XOR, allopurinol, or the mitochondrially targeted antioxidant MitoQ. XO activity was increased in cardiomyocytes from ACF vs. sham rats (24h) without an increase in XO protein. A two-fold increase in LV end-diastolic pressure/wall stress and a decrease in LV systolic elastance with ACF were improved with allopurinol (100 mg/kg) started at ACF induction. Subsarcolemmal state 3 mitochondrial respiration was significantly decreased in ACF and normalized by allopurinol. Cardiomyocytes subjected to 3 hour cyclical stretch resulted in an increase in XO activity and mitochondrial swelling, which was prevented by allopurinol or MitoQ pretreatment. These studies establish an early interplay between cardiomyocyte XO activation and bioenergetic dysfunction that may provide a new target that prevents progression to heart failure in VO.

Keywords

volume overload; oxidative stress; MitoQ; stretch; mitochondria; allopurinol

Introduction

Volume overload (VO) increases diastolic load and results in a progressive eccentric left ventricular (LV) remodeling and systolic dysfunction leading to cardiac failure (1). Currently, there is no medical therapy that halts the progression to heart failure in an isolated

Address reprints: Louis J Dell'Italia, MD, UAB Center for Heart Failure Research, Division of Cardiology, 434 BMR2, 1530 3rd Avenue South, Birmingham, AL 35294-2180, Telephone: (205) 934-3969, Fax: (205) 996-2586, loudell@uab.edu.

VO of aortic or mitral regurgitation (2). We have recently shown that patients with isolated mitral regurgitation have decreased LV systolic function 6 months post-mitral valve repair, despite LV ejection fraction (EF) > 60% prior to surgery (3). Biopsies taken at the time of mitral valve repair demonstrate significant myofibrillar loss with increased xanthine oxidoreductase (XOR), protein nitration, and lipofuscin accumulation in cardiomyocytes, consistent with increased formation of reactive oxygen and nitrogen species (ROS/RNS). Correspondingly, there is also evidence of aggregates of small mitochondria in cardiomyocytes, which is generally considered a response to bioenergetic deficit in cells.

XOR exists as xanthine dehydrogenase and xanthine oxidase (XO), both of which metabolize purines to form uric acid (4). In its oxidase form, XOR produces superoxide and hydrogen peroxide when oxygen is used as an electron acceptor during purine metabolism. Superoxide and hydrogen peroxide can negatively impact multiple metabolic processes in the cardiomyocyte either independently or after reaction with nitric oxide (NO) (5,6). One key target for the actions of ROS/RNS in the cell is the mitochondrion because of its high concentration of reactive proteins and lipids in close proximity to multiple enzymes containing redox active iron and copper (7,8).

Not surprisingly, increasing evidence implicates mitochondrial dysfunction in a broad range of cardiovascular pathologies, many of which are associated with increased ROS/RNS (9–11). Mitochondria are a major source of ROS within the cardiomyocyte, mostly due to the univalent reduction of oxygen to superoxide at complexes I, and III (12,13). Importantly, exposure of mitochondria to ROS/RNS can lead to mtDNA damage that compromise protein synthesis and directly modify mitochondrial proteins (8,12). This in turn can lead to increased mitochondrial ROS production and a vicious cycle can then be established between the generation of ROS from non-mitochondrial sources, bioenergetic dysfunction, and oxidative damage to the organelle. Based upon these concepts we hypothesize that XO activation in VO is intimately involved in the mitochondrial dysfunction associated with this form of hemodynamic stress.

To test these concepts we have used a model of VO by inducing an aortocaval fistula (ACF) in rats. Acutely, ACF causes a three-fold increase in LV end-diastolic pressure and a significant increase in LV chamber diameter, consistent with an increase in LV preload (14). The increased work load associated with ACF is manifested by an increase in the pressure volume area (PVA), suggesting increased myocardial oxygen demand (MVO_2) and ATP consumption (15) and is associated with a decrease in subsarcolemmal mitochcondrial function (16). Thus, in this setting, it is likely that a decrease in the bioenergetic capacity of the mitochondria plays a significant role in the myocardium’s ability to meet increased hemodynamic and oxygen demand.

Previous studies have demonstrated beneficial effects of XO inhibition with allopurinol or oxypurinol in multiple animal models of myocardial disease, such as ischemia (17,18), diabetic cardiomyopathy (19), pacing-induced tachycardia in the dog (20), and in the spontaneously hypertensive rat (21). Volume overload increases the physical stress on the heart due to the elevated diastolic load that increases the stretching force on the heart wall, especially during early diastolic filling (22). Interestingly, acute stretch in the lung increases XO activity in endothelial cells and mediates oxidative tissue damage (23). Further, cardiomyocytes display increased ROS in response to mechanical stretch (24). However, the effect of isolated VO or its potential impact resulting from stretch has not previously been studied in human or animal models and its effects on bioenergetic and cardiac function are unknown. Taken together, these findings suggest that the stretching force associated with VO may induce XO activity resulting in increased oxidative stress in cardiomyocytes.

While the mechanism of XO activation in heart failure is not well understood, it is plausible that mitochondrial-induced oxidative stress can lead to the activation of XO by posttranslational modification of the enzyme. XO is generated from its parent enzyme XDH either by irreversible proteolytic cleavage or transient thiol oxidation within the XOR protein (25,26). In patients with heart failure, ROS have been shown to increase sulfhydryl oxidation and have been shown to increase XO activity (27). To test the hypothesis that oxidative stress in the mitochondrion and XO activation are linked in VO, we have utilized the mitochondrially-targeted antioxidant mitoubiquinone (Mito Q) (28–30). Mito Q has been shown to protect mitochondrial function in a number of cardiovascular models including ischemia-reperfusion, endotoxemia, and cardiac hypertrophy (31–33). In the present study, we demonstrate that allopurinol attenuates the mitochondrial dysfunction associated with VO and that cyclic stretch activates XO through a mechanism dependent on mitochondrial ROS.

Materials and Methods

Animal Preparation

Sprague-Dawley rats (200–250g) at 12 weeks of age were subjected to sham and ACF surgery as previously described in our laboratory (14,16) with and without XO inhibitor allopurinol (100 mg/kg, Sigma), which was started at the time of sham surgery or ACF induction. Separate sets of sham and ACF rats were sacrificed 24 h after surgery for studies of isolated cardiomyocytes (N=5 per group) and heart mitochondria (N=6 per group). Another group of sham and ACF rats were studied for *in vivo* hemodynamic and echocardiographic measurements prior to sacrifice and this tissue was used for protein analysis. To examine the effects of cardiomyocyte stretch on XO activity, 12 week old Sprague-Dawley rats (200–250g) were sacrificed and isolated cardiomyocytes were obtained for *in vitro* stretch studies. This study was approved by the University of Alabama at Birmingham Animal Resource Program.

Hemodynamics and echocardiography

Echocardiography and hemodynamics were performed prior to sacrifice using the Visualsonics imaging system (Vivo 770, Toronto, Canada) combined with simultaneous high-fidelity LV pressure catheter recordings (Millar Inst. Houston, TX). With the rat under isoflurane anesthesia, a high-fidelity LV pressure catheter was advanced into the LV cavity via a right carotid cut-down. Simultaneous LV pressure and echocardiographic dimensions (wall thickness and chamber diameter) were obtained using software included in the Visualsonics system. LV volume was calculated from traced m-mode LV dimensions using the Teicholz formula.

$$V=[7/(2.4+LVID)] \cdot [LVID]^3$$

Where V= volume, LVID= LV internal dimension.

LV wall stress was calculated from traced m-mode LV dimensions and simultaneous LV pressure data using the equation below.

$$LV\ \sigma=[LVP \cdot r]/[2 \cdot LVwt]$$

Where LV σ= LV wall stress, LVP= LV pressure, r= LV chamber radius, LVwt= LV wall thickness.

The LV pressure-volume data were analyzed for LV PVA and stroke work using the Labscribe2 (iWorx System Dover, NH) software package.

Isolation of heart subsarcolemmal mitochondria and activity measurements

Heart subsarcolemmal mitochondria (SSM) were isolated from LV tissue (70mg) as previously described in our laboratory(16,34). The pellet resulting from centrifugation of LV homogenate at 1000×g for 5 minutes (4°C) was discarded. The supernatant was centrifuged at 6000×g for 10min and the resulting pellet was washed twice in isolation buffer and used for respiration measurements.

Oxygen consumption was measured using a Clark-type electrode (Hansatech Instruments, Norfolk, UK). State 2 mitochondrial respiration was initiated upon addition of glutamate/malate (5 mmol/L) as substrates. Respiratory state 3 rate of oxygen consumption (nmol O_2 min^{-1}·mg $protein^{-1}$) was measured in the presence of 1.5 mmol/L ADP and State 4 determined after utilization of 15 μmol/L adenosine diphosphate (ADP).

Isolation of LV myocytes

Cardiomyocytes were isolated from Sham and ACF rats, as described in our laboratory (14,16). Briefly, hearts were perfused with perfusion buffer (120 mmol/L NaCl, 15 mmol/L KCl, 0.5 mmol/L KH_2PO_4, 5 mmol/L $NaHCO_3$, 10 mmol/L HEPES, and 5 mmol/L glucose, at pH 7.0) for 5 min and digested with perfusion buffer containing 2% collagenase II (Invitrogen, Carlsbad, CA) for 30 min at 37°C. The right ventricle, atria and apex were removed before the perfused-heart was minced. The digestion was filtered, washed and cells were pelleted. Only samples with purity and viability (rod-shaped) > 95% or 80%, respectively, were used.

Application of stretch to isolated adult rat cardiomyocytes

Cells (2×10^6/well) were allowed to adhere to laminin coated Flexcell plates (Flexcell International Corp., Hillsborough, NC, USA) in DMEM medium containing 10% FBS, 2 mM glutamine, 10 U/mL penicillin, and 100 mg/mL streptomycin for 2 hours before use. Cells were subjected to cyclical strain (60 cycles/min, 3h) on the Flexcell Strain apparatus (model FX-4000; Flexcell International, Hillsborough, NC, USA) at a level of distension sufficient to promote an increment of approximately 5% in surface area at the point of maximal distension on the culture surface. A group of cells stretched for 3 hours were also subjected to either the mitochondrial ROS inhibitor Mito Q (10 nM or 50 nM) or 250 μM allopurinol. Control cells were prepared on identical culture plates but were not exposed to stretch.

Immunohistochemistry in LV myocardium

Rat hearts were immersion-fixed in 10% neutral buffered formalin and paraffin-embedded. 5μm sections were mounted on slides, deparaffinized in xylene and rehydrated in a graded series of ethanol. After blocking with 1x PBS/1% Casein, overnight incubation at 4°C with either XO antibody (1:1000) or nitrotyrosine antibody (1:1000) Upstate Biotechnology, Inc Lake Placid, NY. Alexa Fluor conjugated secondary antibodies (Molecular Probes, Eugene, OR; 1:500 each) were applied to visualize XO (green) and nitrotyrosine (red) in the tissue. Nuclei were stained (blue) with DAPI (1.5μg/ml; Vector Laboratories, Burlingame, CA). Image acquisition (100× objective, 4000× video-screen magnification) was performed on a Leica DM6000 epifluorescence microscope with SimplePCI software (Compix, Inc., Cranberry Township, PA). Images were adjusted appropriately to remove background fluorescence.

Western blot

Tissue lysate (30 μg protein) was separated on 4–12% Bis-Tris gradient gel (Invitrogen), transferred to a PVDF membrane, then incubated with antibody to either XO (1:1000) Santa Cruz Biotechnology, Santa Cruz, CA, NAPDH oxidase p47 phox subunit (1:1000) Cell Signaling Technology, Inc. Danvers, MA, INOS (1:1500) Santa Cruz Biotechnology, Santa Cruz, CA, β-tubulin (1:2000) Sigma-Aldrich, St. Louis, MO, overnight at 4°C followed by incubation with HRP conjugated secondary antibodies. Membranes were incubated with Chemiluminescent Substrate (Pierce, Rockford, IL) and exposed to X-ray film. Densitometry analysis was performed on XOR expression levels which were normalized to tubulin in Sham vs ACF. NADPH oxidase and iNOS expression were normalized to total protein determined by densitometric analysis from ponceau stained membranes in all groups. Membranes were stained with ponceau stain for 2 mins and then destained in phosphate buffered saline to remove background.

Measurement of XO activity in LV tissue and isolated cardiomyocytes

XO activity was measured using high performance liquid chromatography (HPLC) with electrochemical detection (ESA Coularray). LV free wall tissue or isolated cardiomyocytes were homogenized in RIPA buffer. Before measuring enzymatic activity, endogenous urate was removed by eluting the sample on a Sephadex G-25 column. Xanthine (75μM) was then added, and XO activity assessed by monitoring urate production. The specificity of this detection method for urate production by XO was verified by inhibition of urate formation following allopurinol addition in duplicate samples. Activity was normalized to post column protein concentration determined by bicinchoninic acid (BCA) protein assay for myocardial tissue samples and isolated cells.

Transmission electron microscopy of adult rat cardiomyocytes

Cells were fixed in 25% glutaraldehyde overnight. Cells were then suspended in phosphate buffered saline and carefully removed from the flexcell membrane using a cell scraper. Cells were pelleted and mounted for transmission electron microscopy which was performed by EmLabs Inc. Birmingham, Al.

Statistics

Data are expressed as mean ± SEM. XO activity data was compared using Student's t-test for control/stretched isolated cardiomyocytes and Sham/ACF LV tissue homogenates and isolated cardiomyocytes. A two-way ANOVA with student-Newman-Keuls post hoc test was used for all other comparisons among sham, ACF, Sham + allopurinol and ACF + allopurinol. $P < 0.05$ was considered statistically significant.

Results

Morphometric and Hemodynamic Effects of Allopurinol on Aortocaval Fistula

ACF increases venous return to the heart resulting in a left ventricular VO and diastolic dysfunction evidenced by increased LVEDP and LVED wall stress (σ). At 24 hours after induction of ACF, body weight, heart weight/body weight ratio, or heart rate did not differ among Sham, ACF, Sham + allopurinol, and ACF + allopurinol rats (Table 1). Mean arterial pressure (MAP) was decreased with ACF and was unaffected by allopurinol (Table 1). LV end-diastolic dimension (LVEDD) and LVED volume were increased in ACF vs sham rats and were unaffected by treatment with allopurinol (Table 2). LVED pressure and LVED σ increased in ACF vs. sham rats and were normalized in ACF rats treated with allopurinol (Figure 1). LV ejection fraction did not change with ACF and was unaffected by allopurinol (Table 2).

LV Pressure-Volume Analysis

LV high-fidelity pressure was matched to simultaneous echocardiographic dimensions to generate LV pressure-volume loops. Data collected during a 3–5 sec inferior vena cava occlusion yielded a set of LV pressure-volume loops at multiple LV preloads (Figure 2). Prior to occlusion, the LV pressure-volume area was increased 20% in both ACF and ACF + allopurinol vs. sham rats ($P<0.05$ in both cases), indicative of increased LV work load and oxygen demand. Analysis of the LV end-systolic pressure-volume relationship (ESPVR), a relatively load independent measure of LV contractile function, demonstrated a decrease in LV contractility in the ACF group vs. Sham rats (0.36±0.07 vs 1.48±0.2 mmHg/μl, $P<0.05$), which was significantly improved in ACF + allopurinol rats (0.71±0.07 mmHg/μl) vs ACF rats ($P<0.05$).

XO Activity is Increased in ACF Myocardial Tissue and Isolated Myocytes

Immunohistochemistry from sham and control ACF rats demonstrated extensive XO/XDH distribution in endothelial cells and interstitial cells (Figure 3C) and along Z lines in cardiomyocytes (Figure 3A and B), which is consistent with our previous report in the human heart (3). To determine if XO is activated during ACF, XO activity was measured in both LV homogenates and isolated cardiomyocytes from ACF rats (Figure 4A and B). Cardiomyocyte XO specific activity was approximately 10% of the XO activity in whole LV tissue homogenates after normalization to sample protein content (Figure 4A and B). ACF LV tissue homogenates demonstrated a modest 15% increase in XO activity compared to Sham LV homogenates. Interestingly, XO activity from isolated ACF cardiomyocytes was increased 300% compared to sham cardiomyocytes. This suggests that ACF causes greater XO activation in cardiomyocytes even though other cellular locations of XO such as the endothelium and interstitial cells may contain higher basal levels of the enzyme.

Allopurinol decreases protein nitration in ACF LV myocardium

Western blot analysis of iNOS expression demonstrated no significant change in ACF vs Sham (Figure 5A). However, treatment with allopurinol was associated with increased iNOS expression in both Sham and ACF vs. untreated Sham and ACF rats ($P<0.05$ in both cases). Expression of the NADPH oxidase subunit p47 phox did not significantly differ among all groups (Figure 5A, 5B). Immunohistochemical analysis for nitrotyrosine demonstrated increased staining in ACF left ventricles compared to all other groups (Figure 5D vs 5C, 5D, and 5E). It is of interest that in the ACF group (Figure 5D) the staining was aligned along the Z-lines, suggesting increased nitration with elevated XO.

Effects of ACF on Mitochondrial Function

Oxygen consumption was determined in isolated subsarcolemmal mitochondria (SSM) from all experimental groups (Figure 6). As we reported previously (16), State 3 mitochondrial oxygen respiration was decreased in ACF vs. sham rats (Figure 6). In the current study, allopurinol normalized State 3 mitochondrial respiration in the ACF + allopurinol vs. ACF rats. Allopurinol had no effect on State 2 or State 4 mitochondrial respiration but significantly decreased State 3 respiration in Shams. The reasons for this change are not clear but could be due to effects of allopurinol on the purine salvage pathway leading to a decreased activation of mitochondrial respiration or biogenesis.

Effects of Cardiomyocyte Stretch on XO Activity and Mitochondrial Morphology

VO causes increased myocardial stretch and since this has been reported to increase ROS formation (22), we hypothesized that this could contribute to XO activation. To test this hypothesis, isolated adult rat LV myocytes were plated on laminin-coated Flexcell plates and stretched at 1 Hz at 5% sinusoidal strain for 3 hours. Protein homogenates from

stretched vs. unstretched cardiomyocytes demonstrated an increase in XO activity at 3 hrs after stretch (Figure 7). Pre-treatment with Mito Q in unstretched cells and in cells subjected to 3 hours stretch demonstrated no increase in XO activity with both 10 nM or 50 nM doses of Mito Q. Taken together, these results suggest a cause and effect relationship between isolated stretch and increased cardiomyocyte XO activation that is induced by mitochondrial-derived ROS.

Effect of Mechanical Stretch on Myofibrillar and Mitochondrial Structure

Transmission electron microscopy of stretched cardiomyocytes revealed a marked decrease in myofibrillar density as well as structural disruption of the Z-line (Figure 8). In addition, there was evidence of mitochondrial swelling and loss of electron density of cristae in stretched cells vs. unstretched cardiomyocytes. Z-line structural integrity and mitochondrial morphology were preserved by pre-treatment with allopurinol or Mito Q.

Discussion

Inflammation and oxidative stress produce ROS/RNS through a number of enzymatic systems including XO. It is well known that mitochondria are both targets and sources of oxidative stress, which we have shown in VO results in inhibition of the respiratory chain. This is important since VO produces an increase in pressure-volume area (PVA) as shown in Figure 2, which is known to require higher myocardial oxygen consumption (MVO_2) and ATP consumption (15). We reasoned that this combination of increased energy demand and mitochondrial dysfunction increases the susceptibility of the VO heart to failure. Indeed, we have recently established a novel interaction between bioenergetics and activation of MMPs in the cardiomyocyte of the VO heart (16). This is particularly interesting in the context of XO since its substrates, xanthine and hypoxanthine, are elevated under increased bioenergetic demand and bioenergetic dysfunction. In the current study, we report that VO causes an increase in XO activity in LV tissue and cardiomyocytes without changes in total XO protein, consistent with an oxidative post-translational activation of XO (Figure 4).

Since the activation of XO through this mechanism involves the oxidation of thiols, we reasoned that mitochondrial derived oxidants are an early event that could lead to the activation of XO. To test this hypothesis, MitoQ is used to inhibit mitochondrially-derived ROS in the stretched cardiomyocytes. Indeed, MitoQ prevents both stretch induced-XO activation and mitochondrial swelling and disorganization (Figure 8). These results suggest that mitochondria, which comprise 40% of the cardiomyocyte by volume, may be an important source of ROS and play a regulatory role in XO activation in the VO cardiomyocyte.

The current study also demonstrates loss of myofibrillar integrity in isolated cardiomyocytes subjected to cyclic stretch. We have previously shown that 24 hours of ACF results in increased TNF-α levels (35) and ROS formation and matrix metalloproteinase (MMP) activation (16) within cardiomyocytes. Cytokines, XO, and ROS have been shown to cause MMP activation (36–38) and there is increasing evidence that cardiomyocyte MMP activation is responsible for myosin and troponin degradation during cardiac ischemia reperfusion injury (39,40). In addition, transgenic mice expressing active MMP-2 driven by the α-myosin heavy chain promoter exhibit breakdown of Z-band registration, lysis of myofilaments, and disruption of sarcomere and mitochondrial architecture (41). It is of interest that we have recently demonstrated extensive cardiomyocyte myofibrillar loss in association with increased oxidative stress in the myocardium of VO patients with chronic isolated mitral regurgitation (3). Thus, it is tempting to speculate that mitochondrially derived ROS and XO-mediated MMP activation may play a causative role in the

myofibrillar degeneration that has now been identified in the rat (16), dog (42,43), and human (3) with isolated VO.

Increased cardiomyocyte XO activity with acute ACF is also associated with decreased State 3 maximal bioenergetic capacity of isolated subsarcolemmal mitochondria, which is normalized by allopurinol (Figure 6). Mechanical stretch is associated with increased cardiomyocyte XO activity and abnormal mitochondrial structure that is prevented by allopurinol and MitoQ. NADPH oxidase and uncoupled NOS activation have also been identified in cardiomyocyte stretch (44,45). The current study demonstrates XO activation in a heart failure model may be a direct response to physical stretch. Further, our *in vitro* studies also implicate the mitochondria as a source of ROS by demonstrating that XO activation and mitochondrial and cytoskeletal derangements with stretch can be prevented by MitoQ. Therefore, it is tempting to speculate that XO activation is related to ROS production from mitochondrial structural alterations and that allopurinol and MitoQ may have synergistic effects *in vivo*. These data do not exclude a role for NADPH oxidase and iNOS in contributing to the VO-dependent response to stretch but they do suggest that they are required to interact with both mitochondria and XO to contribute to the pathology.

The *in vivo* and *in vitro* findings of the current study suggest that increased XO activity and mitochondrial oxidative stress are central factors in bioenergetic dysfunction in the face of the increased ATP requirements and MVO_2 of VO. Studies by Hare and coworkers have shown that acute administration of allopurinol decreases the MVO_2 while improving contractile function in patients with dilated cardiomyopathy (46) and in dogs with pacing tachycardia induced heart failure (47), suggesting improved myocardial efficiency. We further speculate that increased levels of ADP and AMP, particularly in the setting of mitochondrial dysfunction, that are degraded to XO substrates hypoxanthine and xanthine, can set up a self-perpetuating cycle by which activated XO produces ROS that damage mitochondria, that in turn causes further ROS production and XO activation (Figure 9). In support of this argument, it is of interest that the acute stretch of VO causes relatively greater XO activation in isolated cardiomyocytes (300%) than in the LV tissue homogenate (15%).

LV ejection fraction is preserved after 24 hours of ACF. However, the LV ESPVR, which provides a load independent index of LV contractility, is depressed in the acute 24 hour ACF, and allopurinol improves both LV contractility and diastolic function (Table 2). It is of interest that increased cardiac ADP levels have been linked to diastolic dysfunction by outcompeting ATP at the actin-myosin crossbridge site and subsequently impairing the relaxation process by delayed ADP dissociation, which is the rate limiting step in cross bridge cycling (48). Indeed, artificially altered ADP levels have been shown to directly correlate with increased LVEDP in the rat heart (49). The beneficial effect on LVED σ is particularly important because wall stress is the driving force for LV hypertrophy in VO (1). Because LV mitochondrial and diastolic function are simultaneously normalized by allopurinol, it is tempting to speculate that allopurinol attenuates ROS-dependent mitochondrial damage and improves diastolic function by improving maximal ADP-stimulated respiratory capacity and decreasing buildup of ADP.

Whether allopurinol improves LV function in acute VO through its effect on mitochondrial respiration cannot be conclusively demonstrated in the current study, since we only measured the respiration of sub-sarcolemmal mitochondria respiration and not intermyofibrillar mitochondrial respiration. In addition, *in vitro* studies demonstrate that XO depresses myofilament sensitivity to calcium and that it co-localizes with nitric oxide synthase-1 in the sarcoplasmic reticulum in the mouse cardiomyocyte, which can regulate excitation-contraction coupling as well as myofilament oxidative damage (50,51).

Specifically, XO inhibition restores ryanodine receptor nitrosylation, reverses diastolic sarcoplasmic reticulum calcium leak, and improves cardiomyocyte contractility in the spontaneously hypertensive heart failure rat (52) and improves the maladaptive changes in calcium cycling proteins associated with LV failure in the pacing tachycardia dog model (53). In the current study, XO protein staining by immunohistochemistry is most concentrated at the Z-line in the cardiomyocyte, which is similar to the findings in the human cardiomyocyte (3). Further, *in vitro* stretch of cardiomyocytes results in loss of myofibrillar structural integrity of the Z-line concurrent with increase XO activity, both of which are prevented with allopurinol or Mito Q. Thus, we cannot rule out an alternative calcium/myofilament mediated mechanism by which allopurinol improves LV contractile performance in this acute VO.

In summary, we have shown that acute VO increases XO activity in heart tissue and isolated cardiomyocytes and that defects in subsarcolemmal mitochondrial respiration and LV dysfunction with VO are reversed by allopurinol. Further, cyclic stretch of cardiomyocytes increases XO activity producing mitochondrial structural defects that are attenuated by allopurinol or MitoQ. Taken together, these studies indicate that XO activation from stretch induced oxidative stress may be central to both bioenergetic and LV dysfunction in acute VO.

Acknowledgments

This study is supported by NHLBI Grants RO1 HL54816 (LJD) and Specialized Center of Clinically Orientated Research in Cardiac Dysfunction P50HL077100 (LJD). BRZ was supported by National Institute of Health grants T 32 HL007918.

List of Abbreviations

ACF	aortocaval fistula
ATP	adenosine triphosphate
ECM	extracellular matrix
LV	left ventricle
LVEDD	LV end-diastolic dimension
LVED σ	LV end-diastolic wall stress
LVEDV	LV end-diastolic volume
LVESD	LV end-systolic dimension
LVES σ	LV end-systolic wall stress
LVESV	LV end-systolic volume
MVO2	myocardial oxygen consumption
PVA	pressure-volume area
SSM	subsarcolemmal mitochondria
VO	volume overload
XO	xanthine oxidase

References

1. Grossman W, Jones D, McLaurin LP. Wall stress and patterns of hypertrophy in the human left ventricle. J. Clin. Invest. 1975; 56:56–64. [PubMed: 124746]

2. Borer JS, Bonow RO. Contemporary approach to aortic and mitral regurgitation. Circulation. 2003; 108:2432–2438. [PubMed: 14623790]

3. Ahmed MI, Gladden JD, Litovsky SH, Lloyd SG, Gupta H, Inusah S, Denney T Jr, Powell P, McGiffin DC, Dell'Italia LJ. Increased oxidative stress and cardiomyocyte myofibrillar degeneration in patients with chronic isolated mitral regurgitation and ejection fraction >60%. J. Am. Coll. Cardiol. 2010; 55:671–679. [PubMed: 20170794]

4. Pacher P, Nivorozhkin A, Szabo C. Therapeutic effects of xanthine oxidase inhibitors: renaissance half a century after the discovery of allopurinol. Pharmacol. Rev. 2006; 58:87–114. [PubMed: 16507884]

5. Ungvari Z, Gupte SA, Recchia FA, Batkai S, Pacher P. Role of oxidative-nitrosative stress and downstream pathways in various forms of cardiomyopathy and heart failure. Curr. Vasc. Pharmacol. 2005; 3:221–229. [PubMed: 16026319]

6. Houston M, Chumley P, Radi R, Rubbo H, Freeman BA. Xanthine oxidase reaction with nitric oxide and peroxynitrite. Arch. Biochem. Biophys. 1998; 355:1–8. [PubMed: 9647660]

7. Moncada S, Higgs EA. The discovery of nitric oxide and its role in vascular biology. Br. J. Pharmacol. 2006; 147:S193–S201. [PubMed: 16402104]

8. Gutierrez J, Ballinger SW, Darley-Usmar VM, Landar A. Free radicals, mitochondria, and oxidized lipids: the emerging role in signal transduction in vascular cells. Circ. Res. 2006; 99:924–932. [PubMed: 17068300]

9. Ramachandran A, Levonen AL, Brookes PS, Ceaser E, Shiva S, Barone MC, Darley-Usmar V. Mitochondria, nitric oxide, and cardiovascular dysfunction. Free Radic. Biol. Med. 2002; 33:1465–1474. [PubMed: 12446203]

10. Di Lisa F, Kaludercic N, Carpi A, Menabo R, Giorgio M. Mitochondria and vascular pathology. Pharmacol. Rep. 2009; 61:123–130. [PubMed: 19307700]

11. Sorescu D, Griendling KK. Reactive oxygen species, mitochondria, and NAD(P)H oxidases in the development and progression of heart failure. Congest. Heart Fail. 2002; 8:132–140. [PubMed: 12045381]

12. Benzi G, Curti D, Pastoris O, Marzatico F, Villa RF, Dagani F. Sequential damage in mitochondrial complexes by peroxidative stress. Neurochem. Res. 1991; 16:1295–1302. [PubMed: 1664494]

13. Fry M, Green DE. Cardiolipin requirement for electron transfer in complex I and III of the mitochondrial respiratory chain. J. Biol. Chem. 1981; 256:1874–1880. [PubMed: 6257690]

14. Ryan TD, Rothstein EC, Aban I, Tallaj JA, Husain A, Lucchesi PA, Dell'Italia LJ. Left ventricular eccentric remodeling and matrix loss are mediated by bradykinin and precede cardiomyocyte elongation in rats with volume overload. J. Am. Coll. Cardiol. 2007; 49:811–821. [PubMed: 17306712]

15. Nozawa T, Cheng CP, Noda T, Little WC. Relation between left ventricular oxygen consumption and pressure-volume area in conscious dogs. Circulation. 1994; 89:810–817. [PubMed: 8313570]

16. Ulasova E, Gladden JD, Zheng J, Chen Y, Pat B, Powell P, Zhmijewski J, Ballinger S, Darley-Usmar V, Dell'Italia LJ. Extracellular matrix loss in acute volume overload causes structural alterations and dysfunciton in cardiomyocyte subsarcolemmal mitochondria. J. Mol. Cell. Cardiol. 2011; 50:147–156. [PubMed: 21059354]

17. Nishizawa J, Nakai A, Matsuda K, Komeda M, Ban T, Nagata K. Reactive oxygen species play an important role in the activation of heat shock factor 1 in ischemic-reperfused heart. Circulation. 1999; 99:934–941. [PubMed: 10027818]

18. Angelos MG, Kutala VK, Torres CA, He G, Stoner JD, Mohammad M, Kuppusamy P. Hypoxic reperfusion of the ischemic heart and oxygen radical generation. Am. J. Physiol. Heart Circ. Physiol. 2006; 290:H341–H347. [PubMed: 16126819]

19. Rajesh M, Mukhopadhyay P, Batkai S, Mukhopadhyay B, Patel V, Hasko G, Szabo C, Mabley JG, Liaudet L, Pacher P. Xanthine oxidase inhibitor allopurinol attenuates the development of diabetic cardiomyopathy. J. Cell Mol. Med. 2009; 13:2330–2341. [PubMed: 19175688]

20. Amado LC, Saliaris AP, Raju SV, Lehrke S, St John M, Xie J, Stewart G, Fitton T, Minhas KM, Brawn J, Hare JM. Xanthine oxidase inhibition ameliorates cardiovascular dysfunction in dogs with pacing-induced heart failure. J. Mol. Cell. Cardiol. 2005; 39:531–536. [PubMed: 15963530]

21. Minhas KM, Saraiva RM, Schuleri KH, Lehrke S, Zheng M, Saliaris AP, Berry CE, Barouch LA, Vandegaer KM, Li D, Hare JM. Xanthine oxidoreductase inhibition causes reverse remodeling in rats with dilated cardiomyopathy. Circ. Res. 2006; 98:271–279. [PubMed: 16357304]
22. Ashikaga H, Covell JW, Omens JH. Diastolic dysfunction in volume-overload hypertrophy is associated with abnormal shearing of myolaminar sheets. Am. J. Physiol. Heart Circ. Physiol. 2005; 288:H2603–H2610. [PubMed: 15708954]
23. Abdulnour RE, Peng X, Finigan JH, Han EJ, Hasan EJ, Birukov KG, Reddy SP, Watkins JE III, Kayyali US, Garcia JG, Tuder RM, Hassoun PM. Mechanical stress activates xanthine oxidoreductase through MAP kinase-dependent pathways. Am. J. Physiol. Lung Cell Mol. Physiol. 2006; 291:L345–L353. [PubMed: 16632522]
24. Pimentel DR, Amin JK, Xiao L, Miller T, Viereck J, Oliver-Krasinski J, Baliga R, Wang J, Siwik DA, Singh K, Pagano P, Colucci WS, Sawyer DB. Reactive oxygen species mediate amplitude-dependent hypertrophic and apoptotic responses to mechanical stretch in cardiac myocytes. Circ. Res. 2001; 89:453–460. [PubMed: 11532907]
25. Della CE, Stirpe F. The regulation of rat-liver xanthine oxidase: Activation by proteolytic enzymes. FEBS Lett. 1968; 2:83–84. [PubMed: 11946275]
26. Stirpe F, Della CE. The regulation of rat liver xanthine oxidase. Conversion in vitro of the enzyme activity from dehydrogenase (type D) to oxidase (type O). J. Biol. Chem. 1969; 244:3855–3863. [PubMed: 4308738]
27. Yücel D, Aydoğdu S, Cehreli S, Saydam G, Canatan H, Seneş M, Ciğdem B, Nebioğlu S. Increased oxidative stress in dilated cardiomyopathic heart failure. Clin. Chem. 1998; 44(1):148–154. [PubMed: 9550572]
28. Ross MF, Prime TA, Abakumova I, James AM, Porteous CM, Smith RA, Murphy MP. Rapid and extensive uptake and activation of hydrophobic triphenylphosphonium cations within cells. Biochem. J. 2008; 411:633–645. [PubMed: 18294140]
29. Murphy MP. Targeting lipophilic cations to mitochondria. Biochim. Biophys. Acta. 2008; 1777:1028–1031. [PubMed: 18439417]
30. Lowes DA, Thottakam BM, Webster NR, Murphy MP, Galley HF. The mitochondria-targeted antioxidant MitoQ protects against organ damage in a lipopolysaccharide-peptidoglycan model of sepsis. Free Radic. Biol. Med. 2008; 45:1559–1565. [PubMed: 18845241]
31. Adlam VJ, Harrison JC, Porteous CM, James AM, Smith RA, Murphy MP, Sammut IA. Targeting an antioxidant to mitochondria decreases cardiac ischemia-reperfusion injury. Faseb. J. 2005; 19:1088–1095. [PubMed: 15985532]
32. Supinski GS, Murphy MP, Callahan LA. MitoQ administration prevents endotoxin-induced cardiac dysfunction. Am. J. Physiol. Regul. Integr. Comp. Physiol. 2009; 297:R1095–R1102. [PubMed: 19657095]
33. Graham D, Huynh NN, Hamilton CA, Beattie E, Smith RA, Cocheme HM, Murphy MP, Dominiczak AF. Mitochondria-targeted antioxidant MitoQ10 improves endothelial function and attenuates cardiac hypertrophy. Hypertension. 2009; 54:322–328. [PubMed: 19581509]
34. Bailey SM, Robinson G, Pinner A, Chamlee L, Ulasova E, Pompilius M, Page G, Chhieng D, Jhala N, Landar A, Kharbanda KK, Ballinger S, Darley-Usmar V. S-adenosylmethionine prevents chronic alcohol-induced mitochondrial dysfunction in the rat liver. Am. J. Physiol. Gastrointest. Liver Physiol. 2006; 291:G857–G867. [PubMed: 16825707]
35. Chen Y, Pat B, Zheng J, Cain L, Powell P, Shi K, Sabri A, Husain A, Dell'Italia LJ. Tumor necrosis factor-alpha produced in cardiomyocytes mediates a predominant myocardial inflammatory response to stretch in early volume overload. J. Mol. Cell. Cardiol. 2010; 49:70–78. [PubMed: 20045005]
36. Okamoto T, Akaike T, Nagano T, Miyajima S, Suga M, Ando M, Ichimori K, Maeda H. Activation of human neutrophil procollagenase by nitrogen dioxide and peroxynitrite: a novel mechanism for procollagenase activation involving nitric oxide. Arch. Biochem. Biophys. 1997; 342:261–274. [PubMed: 9186487]
37. Okamoto T, Akaike T, Sawa T, Miyamoto Y, van der Vliet A, Maeda H. Activation of matrix metalloproteinases by peroxynitrite-induced protein S-glutathiolation via disulfide S-oxide formation. J. Biol. Chem. 2001; 276:29596–29602. [PubMed: 11395496]

38. Okamoto T, Valacchi G, Gohil K, Akaike T, van der Vliet A. S-nitrosothiols inhibit cytokine-mediated induction of matrix metalloproteinase-9 in airway epithelial cells. Am. J. Respir. Cell Mol. Biol. 2002; 27:463–473. [PubMed: 12356580]
39. Sawicki G, Leon H, Sawicka J, Sariahmetoglu M, Schulze CJ, Scott PG, Szczesna-Cordary D, Schulz R. Degradation of myosin light chain in isolated rat hearts subjected to ischemia-reperfusion injury: a new intracellular target for matrix metalloproteinase-2. Circulation. 2005; 112:544–552. [PubMed: 16027249]
40. Wang W, Schulze CJ, Suarez-Pinzon WL, Dyck JR, Sawicki G, Schulz R. Intracellular action of matrix metalloproteinase-2 accounts for acute myocardial ischemia and reperfusion injury. Circulation. 2002; 106:1543–1549. [PubMed: 12234962]
41. Bergman MR, Teerlink JR, Mahimkar R, Li L, Zhu BQ, Nguyen A, Dahi S, Karliner JS, Lovett DH. Cardiac matrix metalloproteinase-2 expression independently induces marked ventricular remodeling and systolic dysfunction. Am. J. Physiol. Heart Circ. Physiol. 2007; 292:H1847–H1860. [PubMed: 17158653]
42. Pat B, Chen Y, Killingsworth C, Gladden JD, Shi K, Zheng J, Powell PC, Walcott G, Ahmed MI, Gupta H, Desai R, Wei CC, Hase N, Kobayashi T, Sabri A, Granzier H, Denney T, Tillson M, Dillon AR, Husain A, Dell'Italia LJ. Chymase inhibition prevents fibronectin and myofibrillar loss and improves cardiomyocyte function and LV torsion angle in dogs with isolated mitral regurgitation. Circulation. 2010; 122:1488–1495. [PubMed: 20876440]
43. Tsutsui H, Spinale FG, Nagatsu M, Schmid PG, Ishihara K, DeFreyte G, Cooper G, Carabello BA. Effects of chronic beta-adrenergic blockade on the left ventricular and cardiocyte abnormalities of chronic canine mitral regurgitation. J. Clin. Invest. 1994; 93:2639–2648. [PubMed: 7911128]
44. Browe DM, Baumgarten CM. Angiotensin II (AT1) receptors and NADPH oxidase regulate Cl^- current elicited by beta1 integrin stretch in rabbit ventricular myocytes. J. Gen. Physiol. 2004; 124:273–287. [PubMed: 15337822]
45. Zhou C, Ziegler C, Birder LA, Stewart AF, Levitan ES. Angiotensin II and stretch activate NADPH oxidase to destabilize cardiac Kv4.3 channel mRNA. Circ. Res. 2006; 98:1040–1047. [PubMed: 16556864]
46. Cappola TP, Kass DA, Nelson GS, Berger RD, Rosas GO, Kobeissi ZA, Marbán E, Hare JM. Allopurinol improves myocardial efficiency in patients with idiopathic dilated cardiomyopathy. Circulation. 2001; 104:2407–2411. [PubMed: 11705816]
47. Ekelund UE, Harrison RW, Shokek O, Thakkar RN, Tunin RS, Senzaki H, Kass DA, Marbán E, Hare JM. Intravenous allopurinol decreases myocardial oxygen consumption and increases mechanical efficiency in dogs with pacing-induced heart failure. Circ. Res. 1999; 85:437–445. [PubMed: 10473673]
48. Zhao Y, Kawai M. Kinetic and thermodynamic studies of the cross-bridge cycle in rabbit psoas muscle fibers. Biophys. J. 1994; 67:1655–1668. [PubMed: 7819497]
49. Tian R, Nascimben L, Ingwall JS, Lorell BH. Failure to maintain a low ADP concentration impairs diastolic function in hypertrophied rat hearts. Circulation. 1997; 96:1313–1319. [PubMed: 9286964]
50. Perez NG, Gao WD, Marban E. Novel myofilament Ca^{2+}-sensitizing property of xanthine oxidase inhibitors. Circ. Res. 1998; 83:423–430. [PubMed: 9721699]
51. Khan SA, Lee K, Minhas KM, Gonzalez DR, Raju SV, Tejani AD, Li D, Berkowitz DE, Hare JM. Neuronal nitric oxide synthase negatively regulates xanthine oxidoreductase inhibition of cardiac excitation-contraction coupling. Proc. Natl. Acad. Sci. U. S. A. 2004; 101:15944–15948. [PubMed: 15486091]
52. Gonzalez DR, Treuer AV, Castellanos J, Dulce RA, Hare JM. Impaired S-nitrosylation of the ryanodine receptor caused by xanthine oxidase activity contributes to calcium leak in heart failure. J. Biol. Chem. 2010; 285:28938–28945. [PubMed: 20643651]
53. Saliaris AP, Amado LC, Minhas KM, Schuleri KH, Lehrke S, St John M, Fitton T, Barreiro C, Berry C, Zheng M, Kozielski K, Eneboe V, Brawn J, Hare JM. Chronic allopurinol administration ameliorates maladaptive alterations in Ca^{2+} cycling proteins and beta-adrenergic hyporesponsiveness in heart failure. Am. J. Physiol. 2007; 292:H1328–H1335.

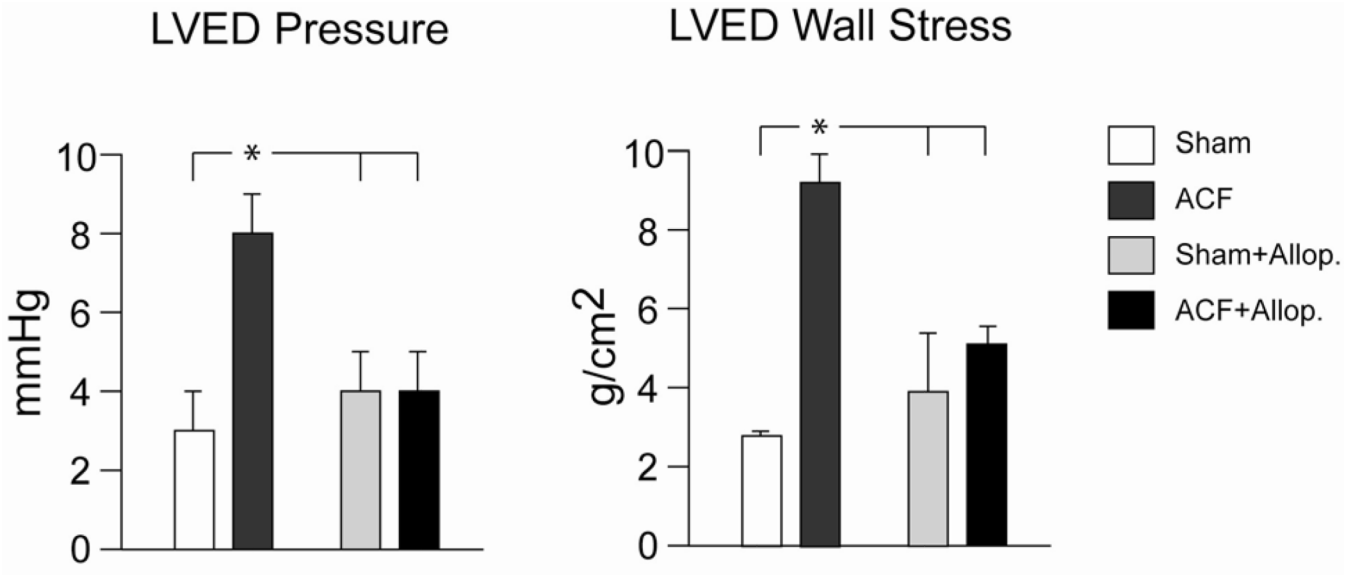

Figure 1. Allopurinol treatment in ACF and its effect on diastolic cardiac function

Sham and ACF rats were studied with and without allopurinol (Allop. 100 mg/kg) initiated at the time of ACF induction. Simultaneous echocardiography and LV high-fidelity pressure catheterization were obtained at 24 hours. LV end diastolic (LVED) pressure and wall stress is increased with ACF and normalized with allopurinol *=P<0.05 vs. sham, sham + Allop., and ACF + Allop.

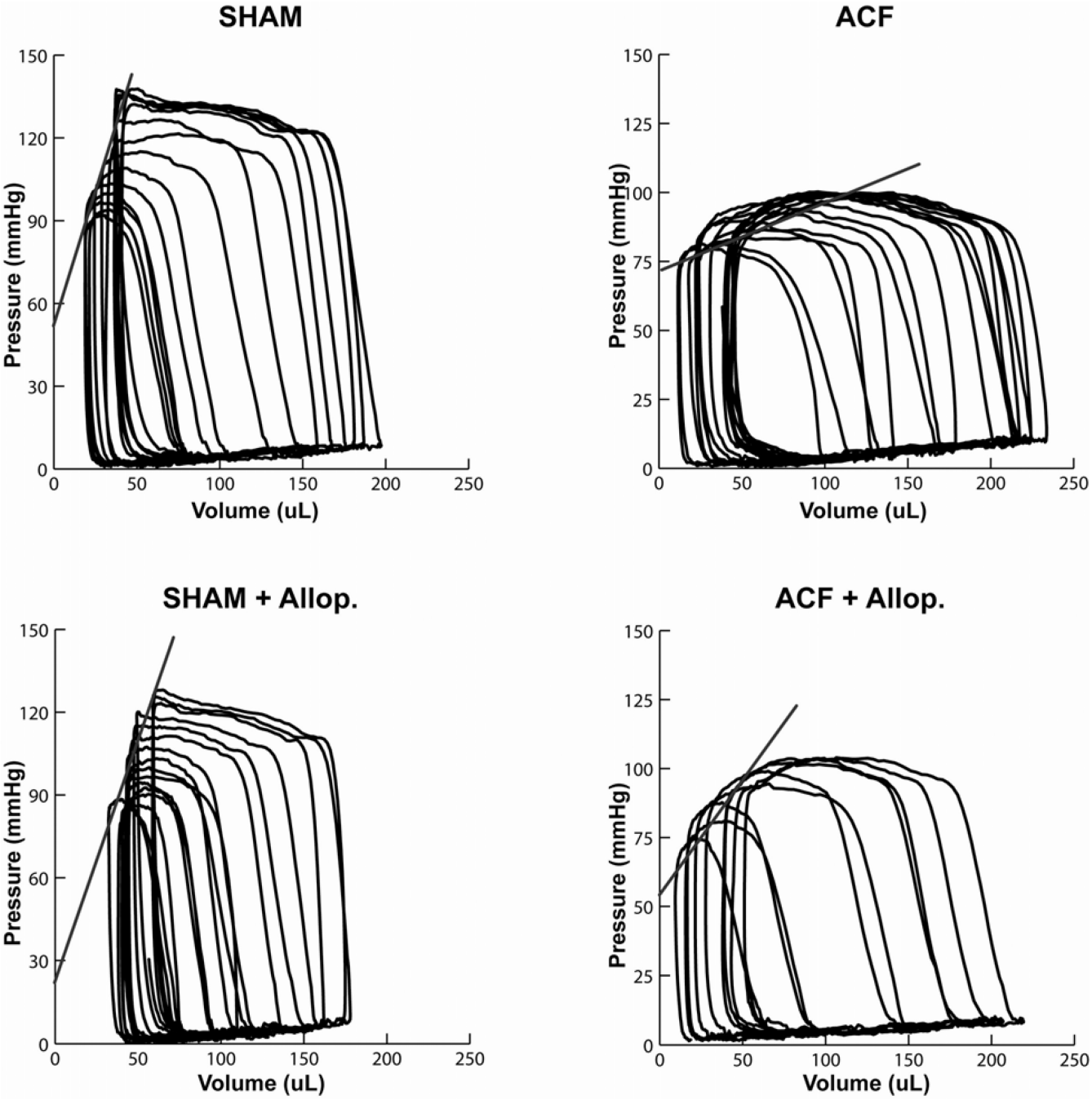

Figure 2. LV End-systolic pressure-volume relationship in ACF and the effects of allopurinol

Representative examples of LV pressure-volume loops generated by a transient inferior vena cava occlusion in Sham (upper left), ACF (upper right), Sham+allopurinol (Allop. lower left), and ACF+allopurinol (lower right). The slope of the LV end-systolic pressure volume relationship is decreased in ACF compared to Sham and significantly improved in ACF +allopurinol (see Table 2, LV ESPVR).

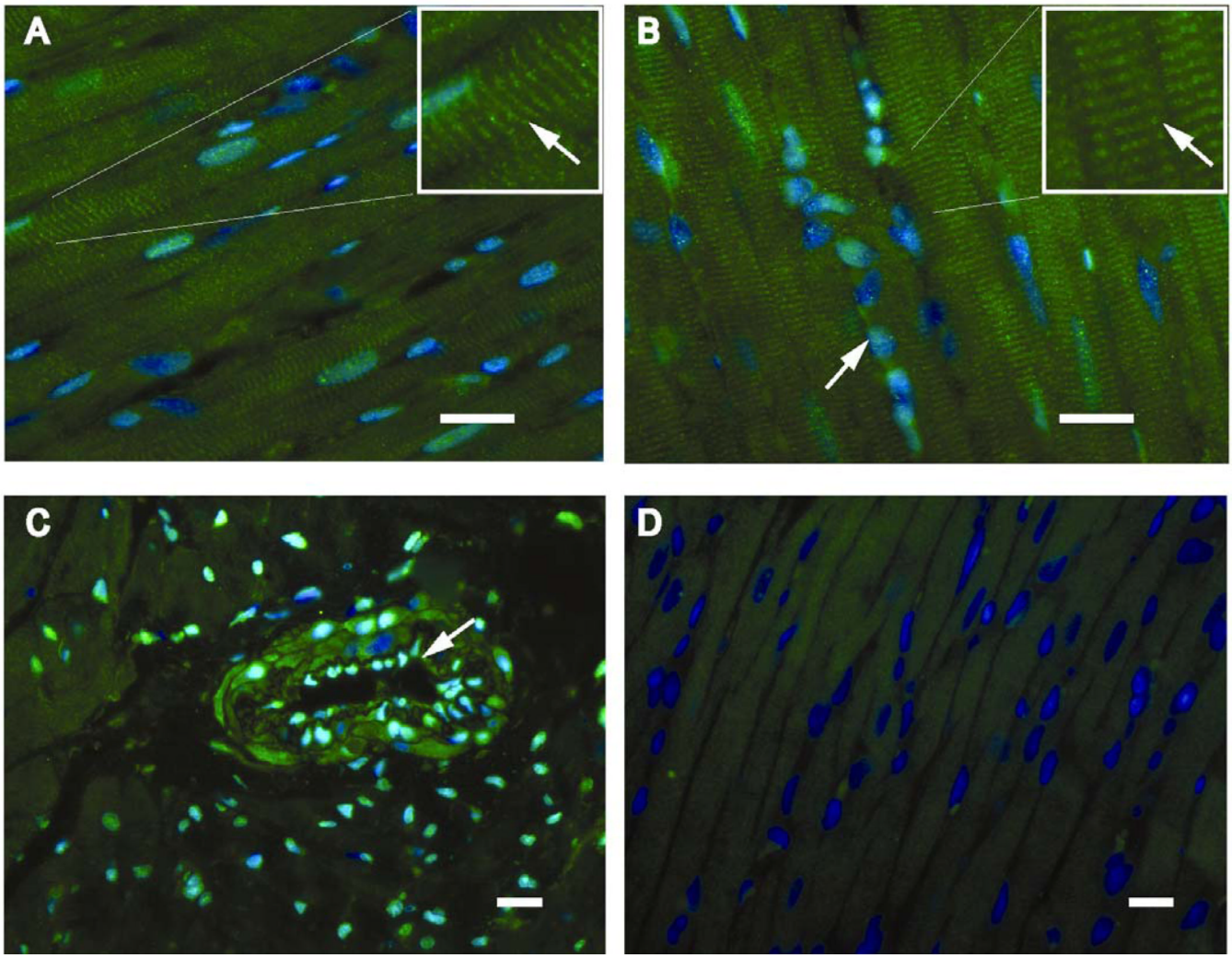

Figure 3. Distribution of XO/XDH cardiomyocytes in sham and 24 hr ACF left ventricles

Immunohistohemistry demonstrates XO/XDH in cardiomyocytes in coordination with Z-lines (arrows), in sham (A) and 24 hour ACF LVs (B) the box in the top right of each panel is a higher magnification view of the same image. In addition, panel B demonstrates XO/XDH in interstitial cells (fibroblasts and endothelial cells) in which nuclei stained with DAPI (blue) take on a more green appearance. In C, cross section of an arteriole in a sham LV demonstrates XO/XDH staining in endothelial cells (arrow) and in smooth muscle cells. The immunoadsorbed antibody (D) demonstrates the blue staining of nuclei with DAPI and lack of XO/XDH staining supporting the specificity of the XO/XDH antibody. White bar represents 20 μm (note different magnifications).

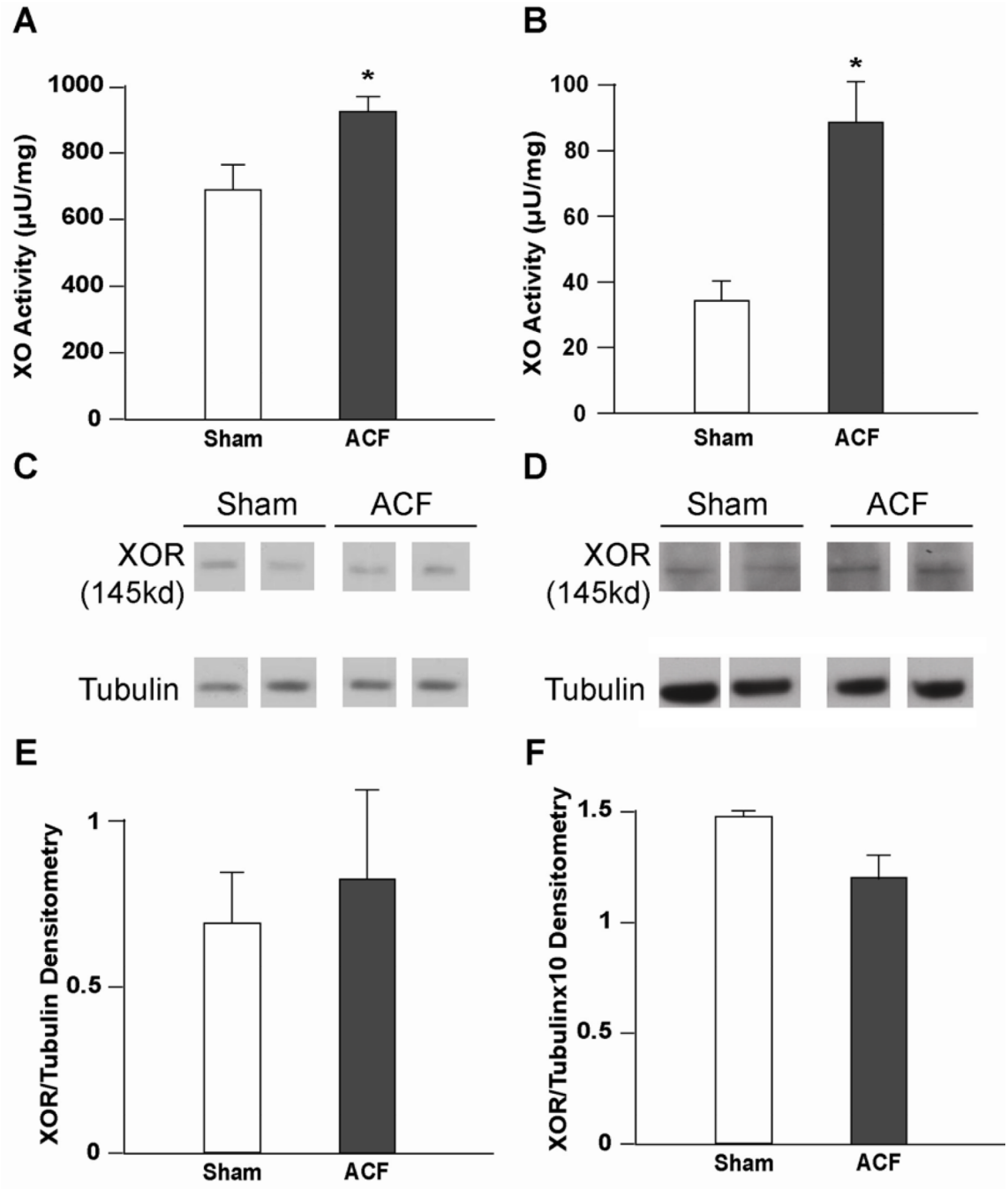

Figure 4. XO activity is predominantly increased cardiomyocytes in 24 hr ACF

XO activity was measured in LV homogenates (A) and isolated cardiomyocytes (B) after 24 hours of ACF. *=P<0.05 vs. sham (n = 4) per group. Protein levels were assessed using an XO/XDH antibody in LV tissue homogenates (sham, n=5 ACF, n=4) (C, densitometry analysis in E) and isolated cardiomyocyte homogenates (n=3) (D, densitometry analysis in F).

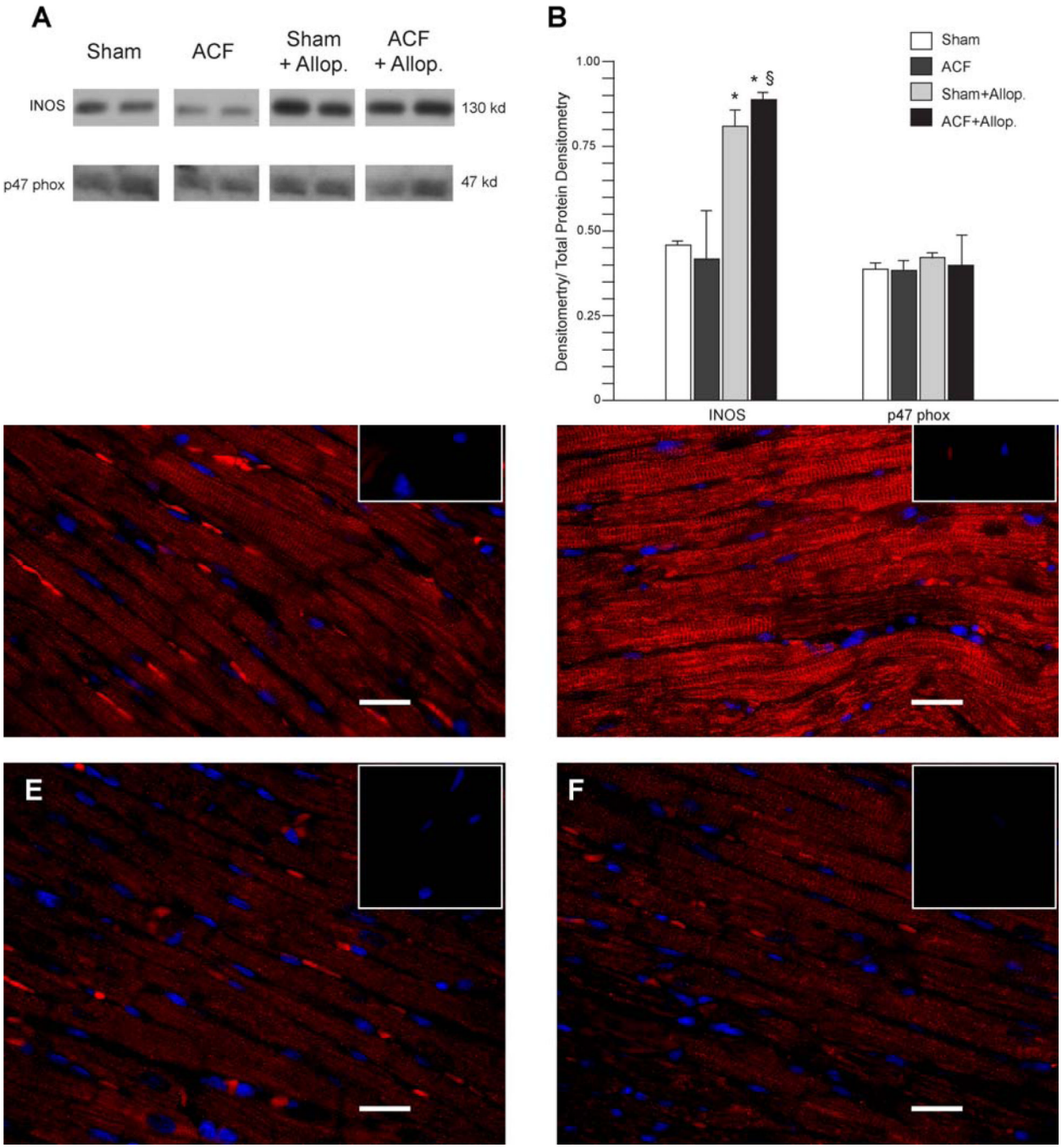

Figure 5. Protein levels of NADPH oxidase, iNOS and protein nitration in LV myocardium

Expression of iNOS and the NADPH subunit p47 phox was measured in LV tissue homogenates by western blot (A) and densitometry analysis was performed (B) n=3 per group. Immunohistochemistry (n=3 per group) demonstrates increased nitrotyrosine (Red) staining in ACF LV tissue (D) compared to Sham (C), Sham+allop. (E) and ACF+allop. (F). Nitrotyrosine appeared to be associated with the Z-line in the ACF in contrast to a more diffuse pattern in all other groups. The inset box (top right box for each panel) is an immunoabsorbed negative for each animal. Nuclei were stained with DAPI (blue) and white bar represents 20 μm. *=P<0.05 vs Sham, §=P<0.05 vs ACF.

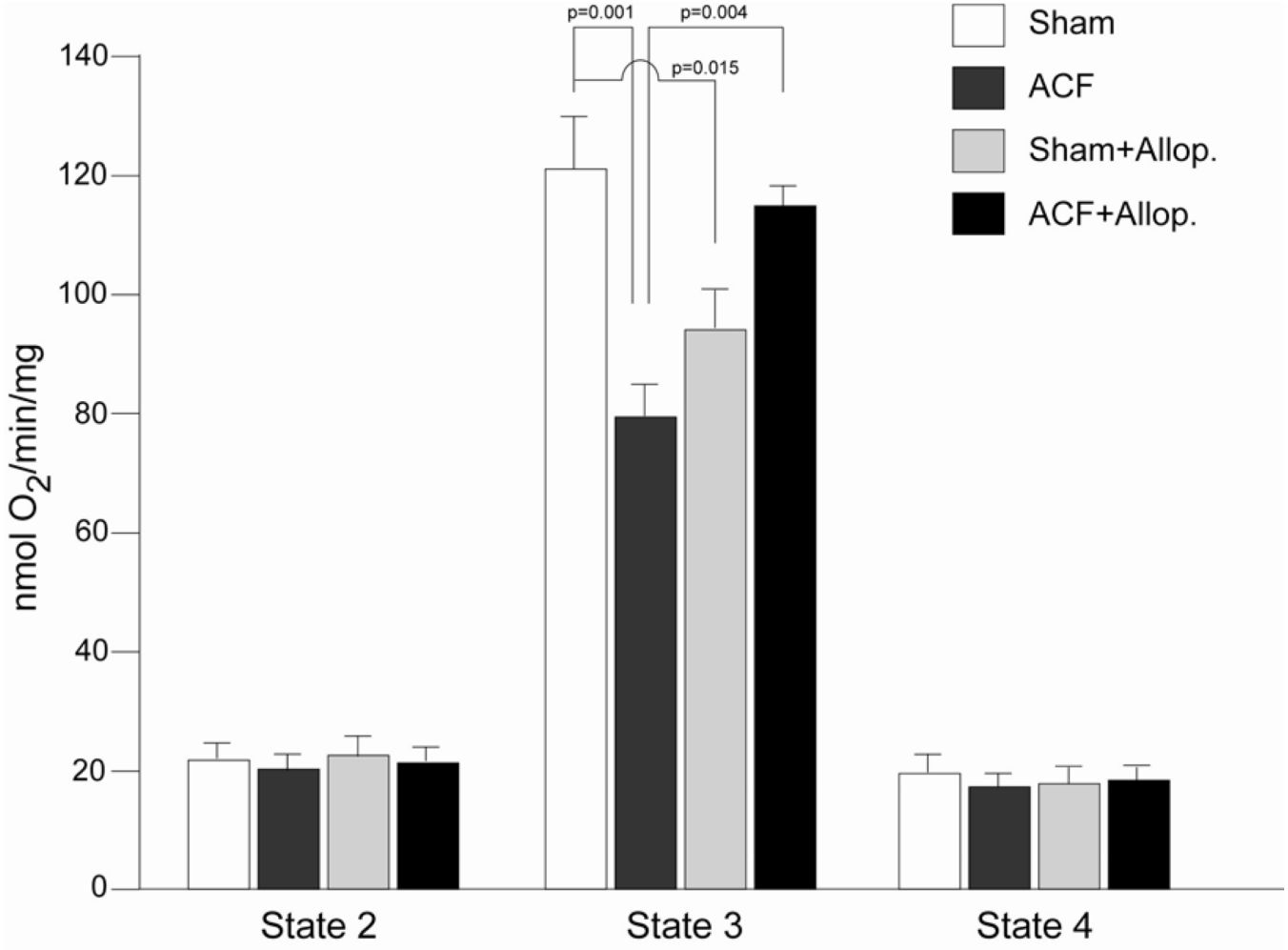

Figure 6. Respiration of isolated subsarcolemmal mitochondria (SSM) in 24 hour ACF and the effects of allopurinol

State 2 and 4 SSM respiration did not differ among all groups. State 3 SSM respiration, a reflection of the mitochondria's maximal ability to consume oxygen, was decreased in ACF vs. shams and significantly improved in ACF + allopurionol, suggesting XO-mediated bioenergetic dysfunction in ACF. n=6 per group.

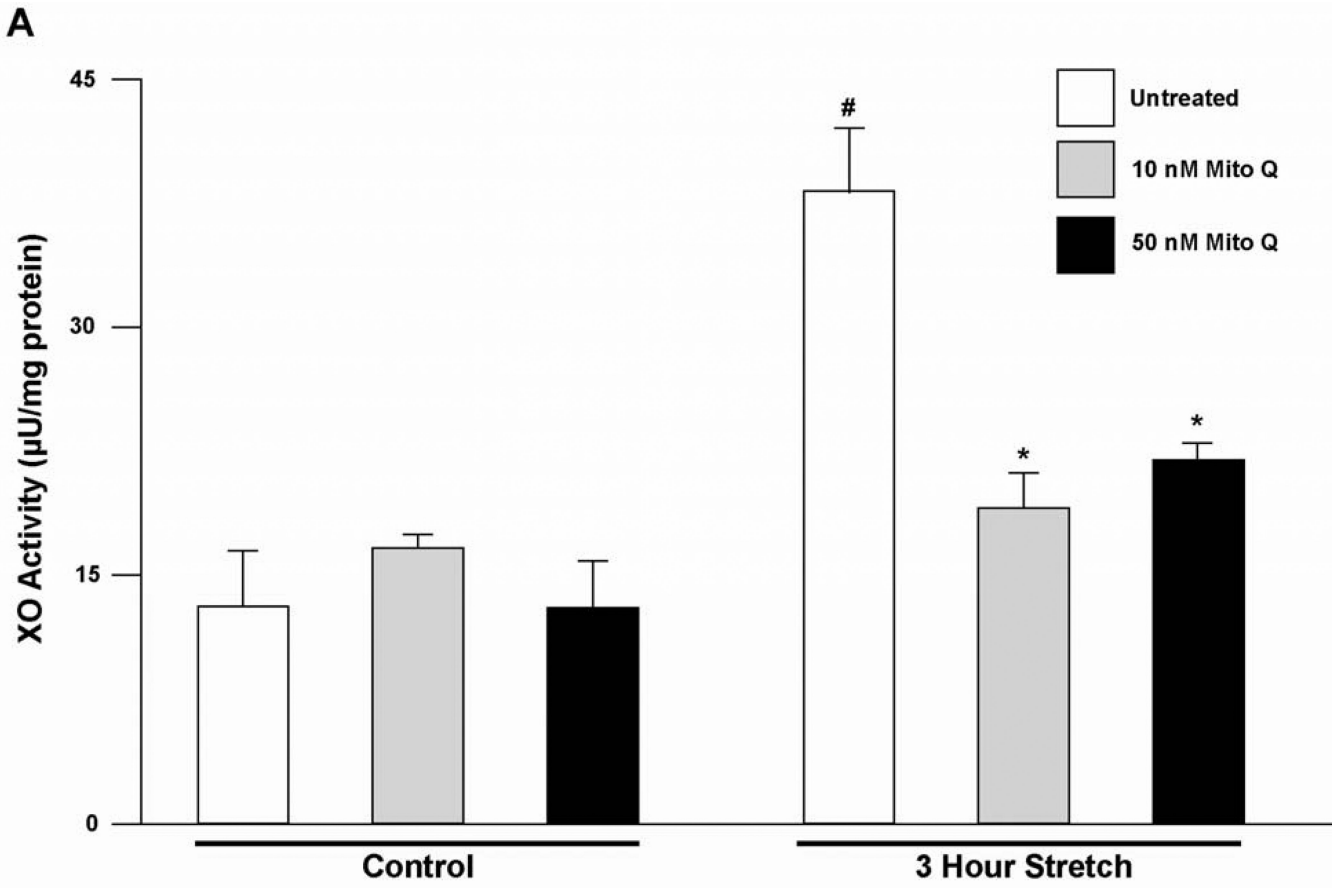

Figure 7. Stretch induces an increase in XO activity by a mitochondrial-derived ROS dependent pathway in adult rat cardiomyocytes

Adult rat cardiomyocytes were cultured in Flexcell culture plates. XO activity was measured in unstretched cells and in cells stretched at 5% for 3 hours. XO activity was also measured after 3 hours of stretch in cells pre-treated with Mito Q, added at the concentrations shown and started 30 min prior to the initiation of stretch (n=5) #=P<0.05 vs. untreated unstretched, *=P<0.05 vs. untreated 3 hour stretch.

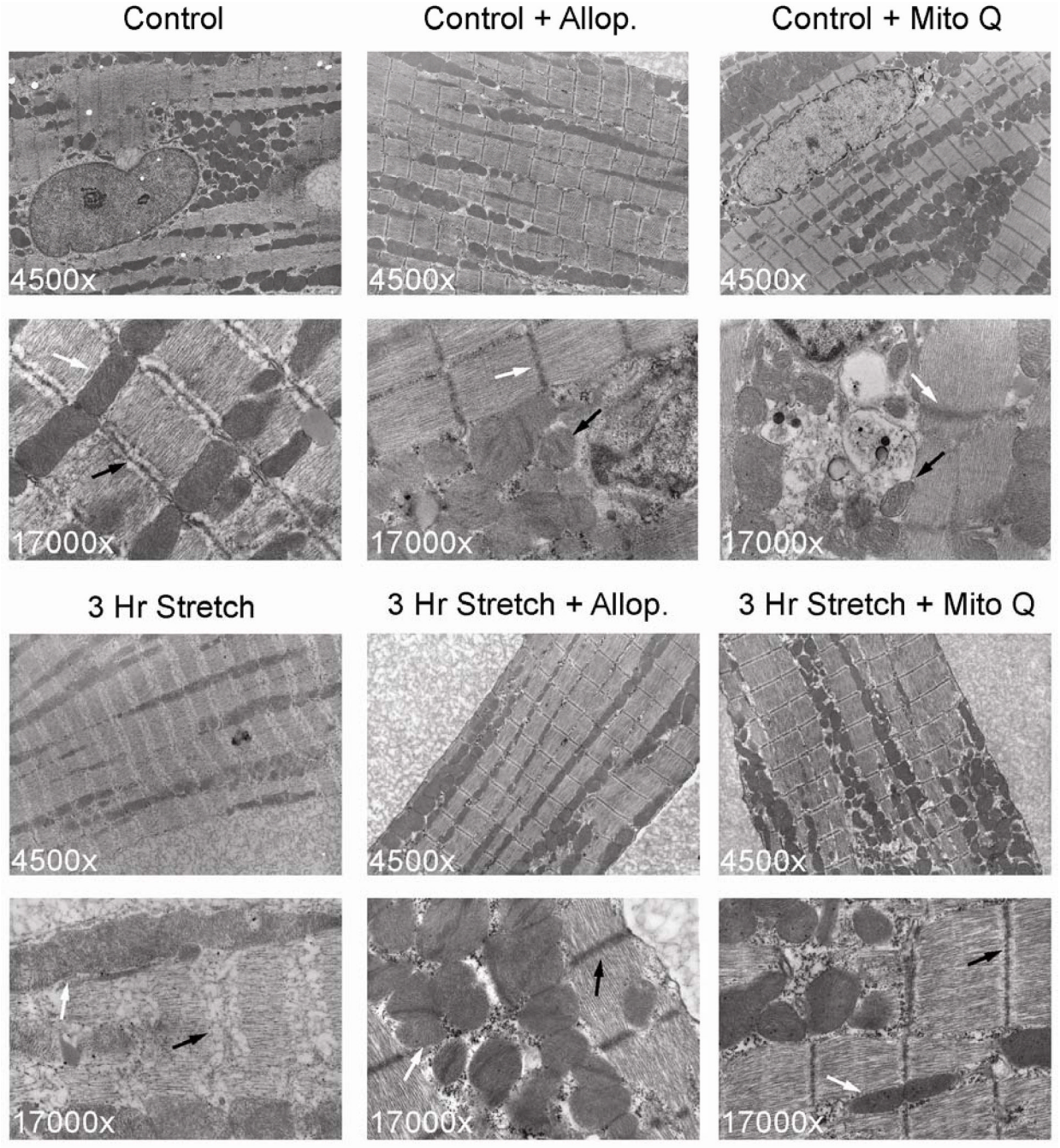

Figure 8. Mechanical stretch is associated with myofibrillar structural abnormalities and mitochondrial swelling in isolated adult rat cardiomyocytes

Upper panels demonstrate unstretched cardiomyocyte control, control + allopurinol (250 μM), control + Mito Q (50 nM) at 4,500× and 17,000×.

Lower panels demonstrated cardiomyocytes subjected to 3 hours of stretch and treated with either 250 μM allopurinol or 50 nM Mito Q. In the 3 hour stretch cardiomyocytes there is marked structural breakdown of myofilaments and Z-line (**black arrows**) and mitochondrial swelling and loss of electron density (**white arrows**) in stretched cells compared to controls. Z-line structural integrity and mitochondrial morphology are preserved by allopurinol or Mito Q pre-treatment.

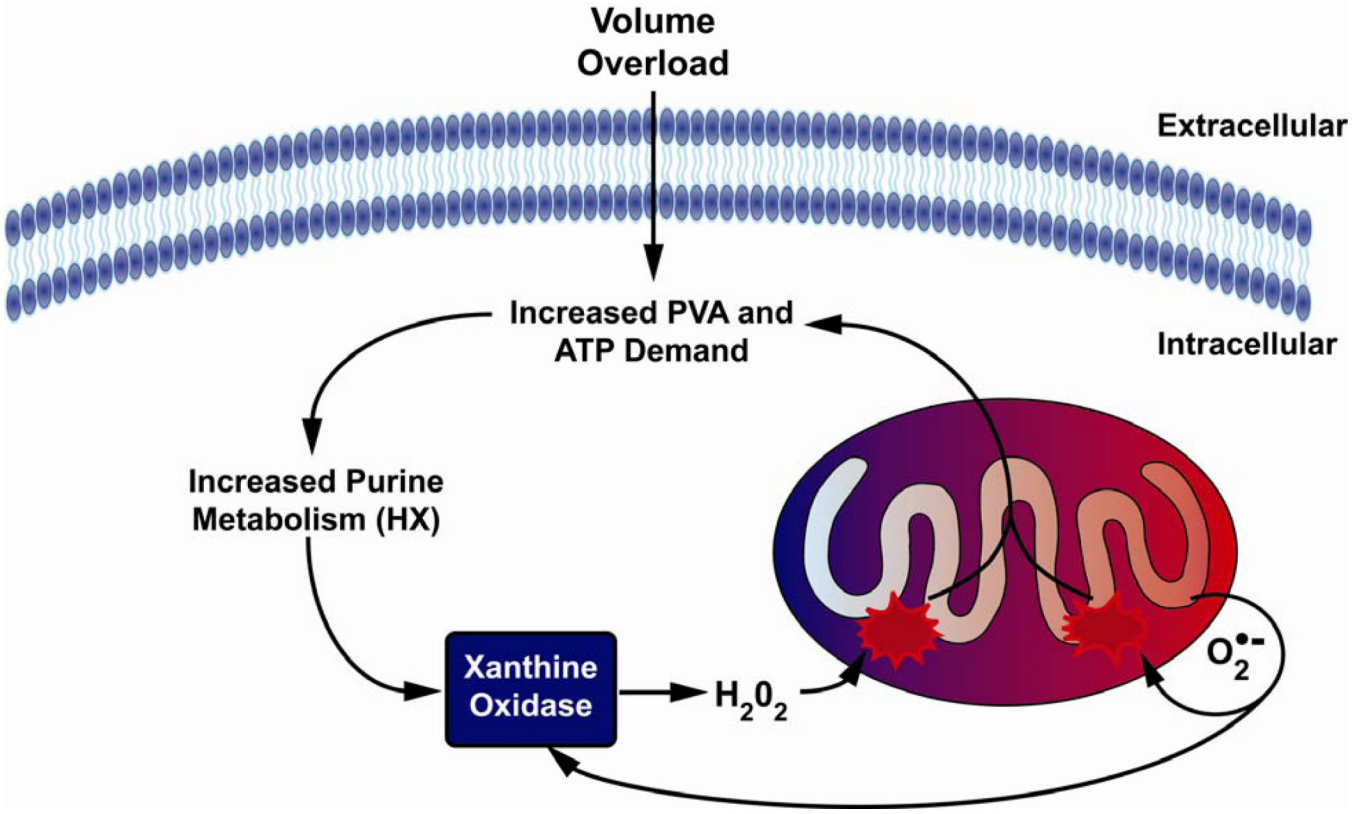

Figure 9. Increased xanthine oxidase activity leads to mitochondrial dysfunction in the VO heart

The increase in pressure volume area (PVA) in VO leads to increased usage of ATP for energy, resulting in increased levels of ADP and AMP. ADP and AMP are then degraded into hypoxanthine (HX) via purine catabolism. XO reacts with HX forming superoxide ($O_2^{\cdot -}$) as a byproduct, which damages mitochondria, leading to bioenergetic dysfunction. $O_2^{\cdot -}$ damages respiratory chain complexes either directly or through interactions with NO, generating peroxynitrite which elicits diverse deleterious effects on the mitochondrion. Collectively, this causes increased electron leak to form more ROS and decreased ATP production. An increase in ROS/RNS and decrease in ATP production feed back into the cycle causing further mitochondrial damage resulting in LV dysfunction.

Table 1

Morphometric Data in shams and ACF rats.

	Sham	ACF	Sham+Allopurinol	ACF+Allopurinol
Body Weight (g)	205±5	203±7	207±7	197±5
Heart Rate (bpm)	374±10	368±6	360±7	362±11
MAP (mmHg)	96±3	62±3*	97±7	70±3*
Heart Weight (g)	0.74±0.02	0.79±0.02	0.75±0.02	0.72±.02
LV Weight (g)	0.51±0.012	0.55±0.01	0.52±0.02	0.49±0.01
Lung Weight (g)	1.16±0.02	1.18±0.03	1.15±0.03	1.07±0.03
Heart/Body Weight	0.0036±0.000083	0.004±0.0001	0.0036±0.0001	0.004±0.00007
N	7	8	6	8

*P<0.5 vs Sham, data = mean ± SE

Table 2

Echocardiographic and hemodynamic data in sham and ACF rats.

	Sham	ACF	Sham+Allopurinol	ACF+Allopurinol
LVESD (mm)	3.54±0.3	3.1±0.3	3.1±0.42	3.5±0.2
LVEDD (mm)	6.4±0.2	6.7±0.3 *	6.4±0.3	7±0.1 *
LVESV (μL)	90±9	92±17	69±14	95±13
LVEDV (μL)	326±17	389±26	308±22	364±18
EF (%)	73±2	77±3	77±4	74±3
LVPWs (mm)	2.8±0.1	3±0.2	3±0.2	2.7±0.1
LVPWd (mm)	1.8±0.1	1.8±0.2	1.8±0.1	1.5±0.03
LVES σ	43±7	23±4 *	34±11	32±4 *
LVED σ	2.5±0.2	8±1.1 *	4±1.5	5±0.6 *§
LV ESPVR	1.48±0.2	0.36±0.07 *	1.62±0.26	0.71±0.07 *§
N	7	8	6	8

LV end-systolic dimension (LVESD), LV end-diastolic dimension (LVEDD), LVES volume (LVESV), LVEDV, LV Ejection Fraction (EF), LVES Posterior wall thickness (LVPWs), LVED Posterior wall thickness (LVPWd) LVES wall stress (σ) LVED σ, LV ES Pressure-Volume

Relationship*= P<0.05 vs Sham,

§P<0.05 vs ACF, data = mean ± SE